Antenna-Coupled Single-Metal Thermocouple Array for Energy Harvesting

Gergo P. Szakmany, Alexei O. Orlov, Gary H. Bernstein, and Wolfgang Porod
Center for Nano Science and Technology, Department of Electrical Engineering
University of Notre Dame
Notre Dame, IN 46556, USA
gszakman@nd.edu

***Abstract*—We study the generation of thermoelectricity by arrays of antenna-coupled nanothermocouples (ACNTCs) in response to long-wave infrared radiation. An ACNTC is constructed from a dipole antenna and a nanoscale thermocouple (NTC). The NTCs are based on a newly discovered thermoelectric effect in single-metal nanostructures with cross-sectional discontinuity. Dependences on antenna array size and polarization are investigated. We show that large arrays of ACNTCs are capable of converting optical energy to measurable electrical signals. This could open the possibility to use such devices for solar energy harvesting in the IR portion of the spectrum, which is inaccessible to photovoltaics.**

Keywords—nanoantenna array, nanothermocouple, Seebeck effect

I. INTRODUCTION

Antenna-coupled nanothermocouples (ACNTCs) for infrared (IR) detection have been studied in the past [1-3]. These devices are constructed from a receiving element (dipole antenna) and a rectifying element (nanothermocouple), and they exploit the wave nature of the IR radiation. The antenna receives the electromagnetic waves, and transfers the optical energy to resonant antenna currents. The dissipated antenna currents heat the hot junction of the thermocouple by Joule heating, and the thermal energy is converted to measurable electrical signal due to the Seebeck effect of the thermocouple. ACNTCs are good candidates for thermal imaging and target tracking applications. Recent simulations show that they are promising candidates for solar energy harvesting [4-7]. Such applications require the cost-effective fabrication of large arrays of ACNTCs. It has been demonstrated that large-scale fabrication of antenna-coupled infrared detector arrays is possible using nanoimprint lithography techniques [8-10]. However, the fabrication of conventional bi-metal nanothermocouple (NTC) arrays was challenging due to the complexity of the device structure and the low alignment tolerance.

Nanothermocouples can be constructed either from two different conductors, or from a single-metal using a newly discovered thermoelectric effect in single-metal nanostructures with cross-sectional discontinuity [11], as shown in Fig. 1. We have shown that when a narrow nanowire segment is inserted between two wider wire segments from the same metal, the resulting difference in the absolute Seebeck coefficients (ASC) leads to a measurable relative Seebeck coefficient (RSC) [11], because the size-dependent reduction of the ASC due to the classical size effect is more pronounced in the narrow wire segment. This effect creates NTC junctions at the size discontinuities, and leads to a thermocouple functionality. The fabrication complexity of single-metal NTCs is significantly reduced compared to conventional bi-metal NTCs, it requires only a single-layer of metal deposition without any alignment. This opens the possibility of fabrication of large array of single-metal thermocouples with nanoimprint lithography.

In this paper, we study the infrared response of antenna arrays constructed from antenna-coupled single-metal thermocouples. Polarization- and array-size-dependent measurements are reported from arrays that contain over 500 individual ACNTCs in a series connection.

II. DESIGN & FABRICATION

A. Antenna design

The antenna is the receiving element; it converts the optical energy to heat by the dissipation of the radiation-induced antenna currents. The geometry of the antenna determines the polarization, frequency response, and directivity of the detector. In this paper, we fabricated ACNTCs with dipole antennas.

In order to maximize the temperature difference between the hot and cold junctions of the ACNTC, the length of the dipole antenna has to appropriately sized for the wavelength of the incident electromagnetic radiation. For 10.6 μm IR radiation, the effective resonant antenna length on a Si/SiO_2 substrate is 2.4 μm, as determined by COMSOL simulations and realized experimentally [12].

The directivity of the antennas is increased by fabricating the devices on top of a metallic ground plane separated by a quarter-wave-thick insulating standoff layer. This ensures that the incident and reflected electromagnetic waves are in-phase at the antenna.

B. Thermocouple design

The hot junction of the NTC senses the temperature increase by the antenna, and the resulting temperature

G.S. gratefully acknowledges financial support from the Notre Dame Joseph F. Trustey Fund for Postdoctoral Scholars.

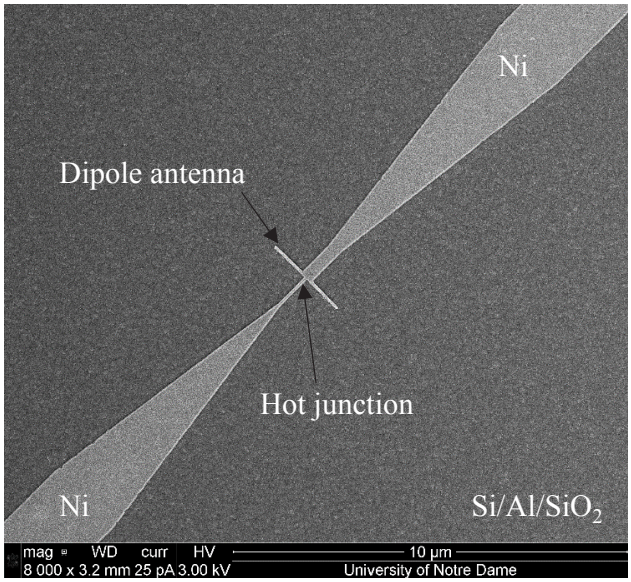

Fig. 1. Scanning electron micrograph of an antenna-coupled single-metal nanothermocouple. The nanothermocouple is constructed from a single layer of Ni nanowires with various cross sections. The width of the narrow wire segment is 50 nm, and the wide wire segment is 300-nm-wide. The dipole antenna is 50 nm wide and 2.4 µm long.

difference between the hot and cold junctions leads to a measurable open-circuit response. For a dipole antenna, a current maximum builds up at its center; therefore, the maximum heat dissipation is also at the center of the antenna. Based on this reasoning, the hot junction is located at the center of the antenna in order to maximize its temperature.

We have previously shown that the relative Seebeck coefficient of single-metal NTCs increases with the width difference between the narrow and wide wire segments [11]. Therefore, we constructed the NTCs from 50 nm and 300 nm wide Ni wire segments, as shown in Fig. 1. Based on our previous work [11], we estimate the value of the RSC to be 1.1 µV/K.

C. ACNTC array design

We constructed antenna arrays from individual ACNTCs as shown in Figs. 2a and 2b. The lead lines of the NTCs are 2-µm-long, and the distance between the columns is 5 µm. The ACNTCs are connected in series by their cold junctions, and 12 devices form a column. A group of four columns form a block that possesses its own read-out interconnects as shown in the schematic in Fig. 2a. This allows antenna-array-size-dependent measurements. It also allows us to bypass defective blocks caused by fabrication error.

D. Fabrication

The antenna array is fabricated on top of a Si wafer coated with a 100-nm-thick Al layer to serve as a ground plane. The devices and the ground plane are separated by a quarter-wave-thick (1.2 µm) SiO_2 layer, deposited by plasma enhanced chemical vapor deposition (PECVD), which also ensures electrical insulation between the devices. The Au bonding pads for the measurements were patterned by optical lithography

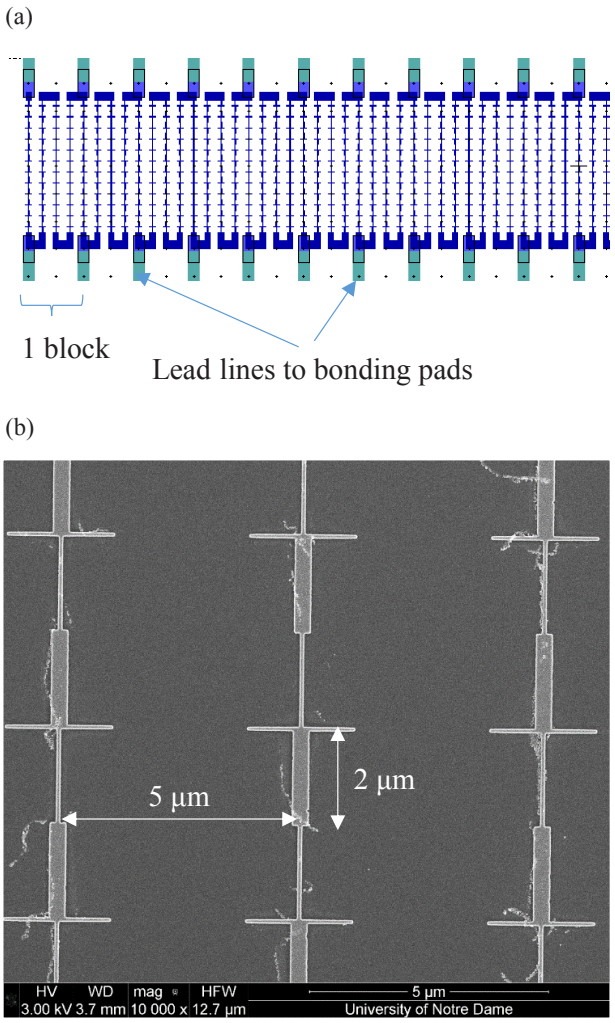

Fig. 2. Array of antenna-coupled single-metal nanothermocouples. (a) Schematic of the ACNTC array connected to the lead lines of the bonding pads. Four columns, containing a total of 48 ACNTCs, form a block to allow array length dependent measurements. (b) Scanning electron micrograph of a segment of the antenna array. The ACNTCs are connected in series at their cold junctions. The lead lines of the thermocouples are 2 µm long, and the separation between the columns is 5 µm.

and formed from a 200-nm-thick Au layer using 10 nm Ti as an adhesion layer.

Fabrication of the antenna-coupled single-metal thermocouple array requires a single step of electron beam lithography and metallization steps. The devices were patterned with a Vistec EBPG 5200 electron beam lithography system [13] into a methyl methacrylate (MMA) and polymethyl methacrylate (PMMA) double-layer resist. The MMA layer was pre-exposed using a deep UV lamp to ensure a large undercut in the resist profile after development that assists in the lift-off process. The patterns were developed in a mixture of MIBK, IPA and MEK [14]. The devices were metallized by 45-nm-thick Ni layer using an electron beam evaporator. Lift-off was performed in 1-methyl-2-pyrrolidinone (NMP).

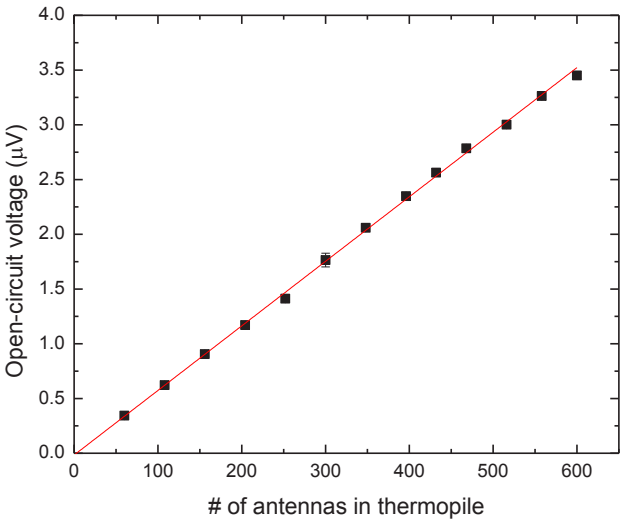

Fig. 3. Measured open-circuit voltage as a function of number of antennas in the array. The measured open-circuit voltage linearly increases.

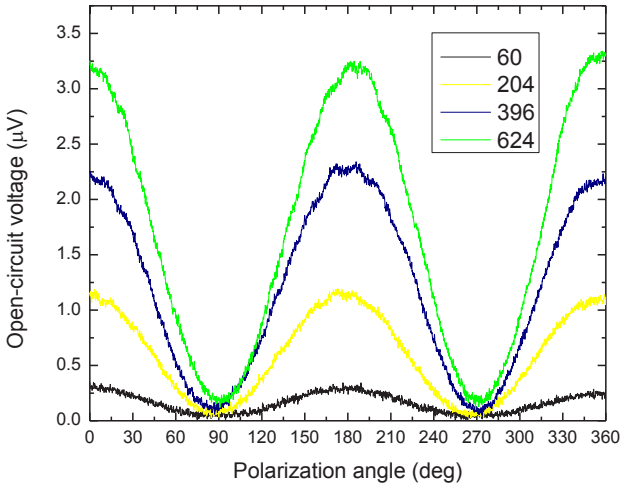

Fig. 4. Measured polarization-dependent response of the antenna arrays with various sizes. The response of the antenna array follows the cosine-square function expected from a dipole antenna.

III. Measurement

For infrared testing, the antenna array was illuminated by a linearly polarized CO_2 laser operating at 10.6 μm (28.3 THz) with an intensity of 1.42 W/cm^2. The laser beam was modulated by a mechanical chopper at a frequency of 960 Hz. The open-circuit voltage response of the array was measured by a custom-made pre-amplifier with a gain of 100 and a lock-in amplifier.

The size of the array covers a 60 μm x 400 μm area between the lead lines of the Au bonding pads. In order to determine the area that is illuminated by the laser beam, its beam shape, transverse extension, and intensity profile were characterized by the widely-used knife-edge measurement technique. We found that 90% of the beam energy of the Gaussian beam is localized to a 500-μm-diameter spot [15].

A. Antenna-array-size-dependent measurements

Antenna-array-size-dependent measurements were performed by varying the number of ACNTCs in the array between 48 and 624. Figure 3 shows the measured open-circuit voltage response as a function of antenna array size. The response follows the thermocouple addition rule; as the number of ACNTCs in the array increases, the measured response increases linearly. This demonstrates that the measured open-circuit voltage response of the antenna array is based on the series connection of individual ACNTCs.

B. Polarization-dependent response

Polarization-dependent response of the antenna array was performed by using a half-wave plate (HWP) to rotate the polarization of the incident electromagnetic IR waves. The measured open-circuit voltages as a function of polarization angle for variously sized arrays are shown in Fig. 4. We measured maximum response when the polarization of the laser beam was parallel to the antenna axis (0 deg, 180 deg, and 360 deg). The minimum response was measured when the polarization of the laser beam was perpendicular to the antenna axis (90 deg and 270 deg). The polarization-dependent response is consistent with the cosine-square function expected for a dipole antenna by classical antenna theory [16].

IV. Summary

Large arrays of antenna-coupled single-metal thermocouples were studied for infrared detection. Polarization-dependent response of the antenna arrays was consistent with the cosine-square function expected for a dipole antenna by classical antenna theory. This proves that the operating principle of the arrays is based on the heating of the hot junction by the radiation-induced antenna current and rectified by the thermocouple. In addition, array-size-dependent measurements show a linear increase of the measured open-circuit voltage as a function of the number of elements in the array. This is consistent with the thermocouple addition rule.

In this paper, we demonstrated that large arrays of ACNTCs function to convert optical energy from the long-wave infrared regime to measurable electrical signals. The use of single-metal NTCs simplifies the fabrication process, allowing the possibility of using cost-effective fabrication techniques, such as nanoimprint lithography. This could open the possibility to use arrays of ACNTCs for solar energy harvesting in the IR portion of the spectrum, which is inaccessible to photovoltaics.

Acknowledgment

The authors acknowledge assistance from the Notre Dame Nanofabrication Facility and the Notre Dame Integrated Imaging Facility.

References

[1] G. P. Szakmany, P. M. Krenz, A. O. Orlov, G. H. Bernstein, and W. Porod, "Antenna-Coupled Nanowire Thermocouples for Infrared

Detection," *IEEE Trans. Nanotechnol.,* vol. 12, no. 2, pp. 163-167, 2013.

[2] P. M. Krenz, B. Tiwari, G. P. Szakmany, A. O. Orlov, F. J. Gonzalez, G. D. Boreman*, et al.*, "Response Increase of IR Antenna-Coupled Thermocouple Using Impedance Matching," *IEEE J. Quantum Electron.,* vol. 48, no. 5, pp. 659-664, 2012.

[3] G. P. Szakmany, A. O. Orlov, G. H. Bernstein, and W. Porod, "Novel Nanoscale Single-Metal Polarization-Sensitive Infrared Detectors," *IEEE Trans. Nanotechnol.,* vol. 14, no. 2, pp. 379-383, 2015.

[4] E. Briones, J. Alda, and F. J. González, "Conversion efficiency of broad-band rectennas for solar energy harvesting applications," *Opt. Express,* vol. 21, no. S3, pp. A412-A418, 2013.

[5] E. Briones, J. Briones, A. Cuadrado, J. C. Martinez-Anton, S. McMurtry, M. Hehn*, et al.*, "Seebeck nanoantennas for solar energy harvesting," *Appl. Phys. Lett.,* vol. 105, no. 9, p. 093108, 2014.

[6] E. Briones, A. Cuadrado, J. Briones, R. Díaz de León, J. C. Martínez-Antón, S. McMurtry*, et al.*, "Seebeck nanoantennas for the detection and characterization of infrared radiation," *Opt. Express,* vol. 22, no. S6, pp. A1538-A1546, 2014.

[7] A. Cuadrado, E. Briones, F. J. González, and J. Alda, "Polarimetric pixel using Seebeck nanoantennas," *Opt. Express,* vol. 22, no. 11, pp. 13835-13845, 2014.

[8] M. Bareiss, P. M. Krenz, G. P. Szakmany, B. N. Tiwari, D. Kalblein, A. O. Orlov*, et al.*, "Rectennas Revisited," *IEEE Trans. Nanotechnol.,* vol. 12, no. 6, pp. 1144-1150, 2013.

[9] M. Bareiß, A. Hochmeister, G. Jegert, U. Zschieschang, H. Klauk, R. Huber*, et al.*, "Printed array of thin-dielectric metal-oxide-metal (MOM) tunneling diodes," *J. Appl. Phys.,* vol. 110, no. 4, p. 044316, 2011.

[10] M. Bareiß, F. Ante, D. Kälblein, G. Jegert, C. Jirauschek, G. Scarpa*, et al.*, "High-Yield Transfer Printing of Metal–Insulator–Metal Nanodiodes," *ACS Nano,* vol. 6, no. 3, pp. 2853-2859, 2012.

[11] G. P. Szakmany, A. O. Orlov, G. H. Bernstein, and W. Porod, "Single-Metal Nanoscale Thermocouples," *IEEE Trans. Nanotechnol.,* vol. 13, no. 6, pp. 1234-1239, 2014.

[12] G. P. Szakmany, A. O. Orlov, G. H. Bernstein, and W. Porod, "Polarization-Dependent Response of Single- and Bi-Metal Antenna-Coupled Thermopiles for Infrared Detection," no. under review.

[13] www.nd.edu/~ndnf.

[14] G. H. Bernstein, D. A. Hill, and W. P. Liu, "New high‐contrast developers for poly(methyl methacrylate) resist," *J. Appl. Phys.,* vol. 71, no. 8, pp. 4066-4075, 1992.

[15] B. N. Tiwari, P. J. Fay, G. H. Bernstein, A. O. Orlov, and W. Porod, "Effect of Read-Out Interconnects on the Polarization Characteristics of Nanoantennas for the Long-Wave Infrared Regime," *IEEE Trans. Nanotechnol.,* vol. 12, no. 2, pp. 270-275, 2013.

[16] C. A. Balanis, *Antenna Theory: Analysis and Design*, 3rd ed. Hoboken, NJ: John Wiley & Sons, Inc. , 2005.